Original scientific paper

Improvement of the corrosion resistance of electrodeposited Zn-Fe by sol-gel conversion films

Céline Arrighi[1,2], Yoann Paint[3], Catherine Savall[2], Juan Creus[2] and Marjorie Olivier[1,3✉]

[1]*University of Mons-UMONS, Faculty of Engineering, Materials Science Department, Place du Parc 20, 7000 Mons, Belgium*
[2]*Laboratoire des Sciences de l'Ingénieur pour l'Environnement (LaSIE) UMR CNRS 7356 - La Rochelle University, Av. Michel Crépeau , 17042 La Rochelle, France*
[3]*Materia Nova ASBL, Avenue Copernic 1, 7000 Mons, Belgium*

Corresponding author: ✉marjorie.olivier@umons.ac.be; Tel.: +32 65 37 44 31

Abstract

An aqueous hybrid inorganic/organic sol-gel solution composed of tetraethylorthosilicate (TEOS), methyltriethoxysilane (MTES) and (3-glycidyloxypropyl)trimethoxysilane (GPTMS) was applied on ZnFe (14 wt.% Fe) electrodeposited on steel as a sacrificial layer. Two precursor contents were studied: 10 (SG10) and 30 % (SG30). First, the morphology and thickness of the films were assessed by Scanning Electron Microscopy (SEM) observations. They revealed the presence of micro-cracks in the films without alkaline surface preparation due to the pyramidal shape of the ZnFe deposit. Then, the corrosion resistance of the systems was determined by Electrochemical Impedance Spectroscopy (EIS) and Neutral Salt Spray (NSS) test. All results indicated an improvement in the corrosion resistance thanks to the presence of the SG films. However, the protection provided by the SG10 film did not permit to durably protect the ZnFe deposit. The combination of surface preparation and a SG30 film provided promising protection to the ZnFe deposit with an increase of the low-frequency modulus and a delay in corrosion product appearance during the NSS test.

Keywords
Electrochemical impedance spectroscopy; zinc alloys; aqueous based solution

Introduction

Zn-Ni (12-14 wt.% Ni) electrodeposits are commonly used as sacrificial coatings to protect steel from corrosion [1,2]. However, researchers tend to focus on eco-friendlier alternatives because of the toxicity of nickel salts [3]. Zn-Fe electrodeposits could be potential candidates for the replacement of Zn-Ni ones [4–10]. Nevertheless, it is essential to improve the corrosion resistance of Zn-Fe deposits in order to achieve the same performance as Zn-Ni coatings. Sol-gel (SG) films, and particularly hybrid inorganic/organic ones, have been used for years to limit the corrosion of metallic systems. This solution was extensively studied for Zn coatings, but less information can be found regarding Zn alloys and particularly Zn-Fe ones.

Su *et al.* [11] compared the effect of an inorganic (TEOS) and a hybrid inorganic/organic (TEOS + GPTMS) SG films deposited on galvanized steel. They studied the influence of SG films on the corrosion resistance and the paint adhesion of the systems. SEM observations indicated that both SG films follow the morphology of the substrate (which was skin-passed). However, micro-cracks were observed for the inorganic SG film. The absence of cracks for the hybrid SG film was attributed to the presence of GPTMS. The Neutral salt spray (NSS) test revealed a delay in the appearance of corrosion products thanks to the presence of SG films with better performance for the hybrid SG film. Corrosion products were first observed on the micro-cracks, explaining the better results obtained for the hybrid SG film. Electrochemical tests were also performed, indicating a decrease in the corrosion current density thanks to SG films (from 6.00 µA cm^{-2} for galvanized steel to 3.8 µA cm^{-2} for inorganic film and 0.12 µA cm^{-2} for the hybrid film). Electrochemical impedance spectroscopy (EIS) measurements were performed in 0.1 M NaCl, and an electrical equivalent circuit (EEC) was used to represent the behaviour of the system. This EEC was composed of the electrolyte resistance; the SG film was represented by the pore resistance (R_{pore}) and the coating CPE ($Q_{coating}$) and the charge transfer at the interface was represented by the charge transfer resistance (R_{ct}) and the double layer CPE (Q_{dl}). All results indicated an improvement of the corrosion resistance by using the hybrid SG film with an increase in the charge transfer and the pore resistances. Other authors obtained similar conclusions with inorganic or hybrid SG films, combined or not with corrosion inhibitors, on zinc [12–14], electrodeposited zinc [15], or galvanized steel [11,16–25]. Regarding zinc alloys, Dos Santos [26] studied the influence of bis[3-(triethoxysilyl)propyl] tetrasulfide (BTESPTS) or 1,2-bis(triethoxysilyl) ethane (BTSE) + BTESPTS SG films combined with Ce or La conversion layers, on the corrosion resistance of electrodeposited Zn-Fe (2 wt.%). EIS measurements in 0.05 M NaCl indicated an increase of the low-frequency modulus for the systems combining SG and corrosion inhibitors and systems with only conversion layers.

SG can be prepared using alcohols since most precursors are non-miscible with water. However, it is possible to obtain aqueous SG. Fedel *et al.* [16,17,20,27,28] published several studies with this kind of SG applied on galvanized steel in order to optimize the system (curing parameters, the addition of clay, etc). The matrix consisted of a mixture of TEOS, MTES and GPTMS. They used acidic catalysis with hydrochloric acid and 10 % in precursors. C. Motte [29] studied the impact of an aqueous SG film composed of 10 % TEOS, MTES and GPTMS on the corrosion resistance of galvanized steel. She also incorporated clay (modified or not by cerium) in her work. A. Nicolay [30] studied the influence of the precursors ratio (10, 20 and 30 %) and applied SG films on stainless steel. In this study, an aqueous SG was chosen to avoid using volatile solvents to obtain an eco-friendlier system. The aim of this study is to determine the corrosion resistance improvement brought by SG films deposited on ZnFe coated steel.

Experimental

The substrate consisted of ZnFe (14 wt.% Fe) coated ST37 steel. A 15 µm ZnFe deposit was obtained by electrodeposition from an alkaline additive-free bath composed of 6.6 M of potassium hydroxide (Alfa Aesar), 0.3 M of zinc oxide (VWR Chemicals) and 0.075 M of ferrous gluconate (Alfa Aesar) [4,31] maintained at 25 °C. The pulsed current was used with the following parameters: t_{on} 4 ms, t_{off} 16 ms and j_p 125 mA cm^{-2} [31]. The roughness R_a of the bare electrodeposited ZnFe coating was measured with a NanoJura optical profiler. A R_a value of 1.3 ± 0.2 µm was obtained.

Sol-gel solutions were obtained by mixing demineralized water and three precursors: TEOS (VWR Chemicals), MTES (Alfa Aesar) and GPTMS (Aldrich). Two solutions containing 10 wt.% (SG10) or

30 % in precursors (SG30) were prepared. The composition of each matrix is given in Table 1. Pluronic123 (P123, Aldrich) was added (0.03 wt.%) to improve the wettability of the solution on ZnFe deposits. The pH of the solution was adjusted at 3.5-4 with acetic acid (VWR Chemicals).

Table 1. *Composition and dry extract of the two SG*

	Content, wt.%	
	SG10	SG30
Demineralized water	90	70
TEOS	3.3	10
MTES	3.3	10
GPTMS	3.3	10
Dry extract	4.7 ± 0.1	14.0 ± 0.6

The viscosity of SG solutions was determined with Anton Paar MCR 302 equipment. Shear stress (τ) in the function of the shear rate ($\dot{\gamma}$) graphs were recorded at 25 °C with a shear rate varying from 0 to 1000 s^{-1} for a scan duration of 10 minutes. All SG solutions showed a Newtonian behaviour, and their viscosity was indicated by the slope of the graph $\tau = f(\dot{\gamma})$. After 24 h of stirring, the viscosities of SG10 and SG30 solutions were respectively 1.39 mPa s and 3.00 ± 0.03 mPa s.

Surface preparation was used in some cases, consisting of an immersion of the samples for 30 s in a 10 g L^{-1} alkaline commercial Gardoclean® solution maintained at 50 °C. Samples were then rinsed with demineralized water and dried. SG films were deposited on ZnFe coated steel by dip-coating with a KSV Nima 2 equipment. The withdrawal rate was 500 mm min^{-1}. Systems were then cured at 180 °C for 1 h in a ThermoScientific oven. These curing parameters were optimized by A. Nicolay in previous work [30].

The contact angle between a demineralized water droplet and the different systems (bare ZnFe and ZnFe + SG) was measured to determine the effect of the sol-gel film on the hydrophobicity of the sacrificial layer. The test was performed with a Kruss DSA 10-MK2 equipment with a droplet volume of 1 µL.

The corrosion resistance of the systems was assessed by electrochemical measurements (Solartron Analytical ModuLab) and by Neutral Salt Spray (NSS, Q-FOG SSP600) test. Regarding electrochemical tests, a three-electrode system was used. The reference electrode was a Saturated Calomel Electrode (SCE), the counter-electrode was a platinum grid, and the working electrode was the substrate (1 cm² exposed). A flat cell containing 300 mL of 0.1 M NaCl (VWR Chemicals) was used. The pH of the electrolyte was adjusted at pH 7 with a NaOH solution in order to perform experiments with the same initial pH. The Open Circuit Potential (OCP) of samples was measured and EIS was performed every 6 h until 3 days and then every 12 h until 7 days of immersion. EIS was done with an rms amplitude voltage of 10 mV in the frequency range $10^5 – 10^{-2}$ Hz. Bare ZnFe and ZnFe + SG10 (with and without Gardoclean®) were immersed for 3 days, while ZnFe + SG30 (with and without Gardoclean®) were immersed for 7 days. Experiments were reproduced to obtain two consistent results.

Bare ZnFe and ZnFe + SG were exposed to the NSS test following ISO 9227 standard. 3M tape was used to mask one side of the samples and their edges. A 7 cm² area was exposed. Three samples of each condition were placed in a Q-FOG SSP600 climatic chamber maintained at 35 °C and exposed to a 50 g L^{-1} NaCl solution. Pictures of the samples were taken after 1, 2, 3, 7 and 14 days of exposure.

The coverage of SG films on ZnFe deposits was assessed by SEM observations on the surface and the cross-sections (obtained by cryofracture) of the samples. A Hitachi SU8020 equipment was used.

SEM observations were also coupled with EDX measurements to analyse corrosion products formed on the surface of the samples, in terms of morphology and composition.

This study focuses only on ZnFe deposits since zinc and/or galvanized steel have already been studied with this kind of SG film with promising results.

Results and discussion

Characterization of the coated systems

Table 1 presents the SEM observations of the surface and the cross-section of ZnFe deposits with SG10 and SG30 films, with and without Gardoclean® surface preparation. The surface of the ZnFe electrodeposit was covered with all SG films and ZnFe pyramids could still be observed. However, in the absence of Gardoclean® surface preparation (Figures 1(a) and (b)), some cracks were visible at the bottom of the pyramids, indicating that the SG films could not accommodate the morphology of the ZnFe deposit. When a Gardoclean® surface preparation is performed before the application of SG films (Figures 1(c) and (d)), an improvement was observed with the absence of cracks. SG30 film seemed thicker than SG10 one, especially in the valleys of the ZnFe deposit. This would be consistent with their difference in terms of viscosity. Indeed, the thickness of the SG film can be calculated by the Landau-Levich relation (1).
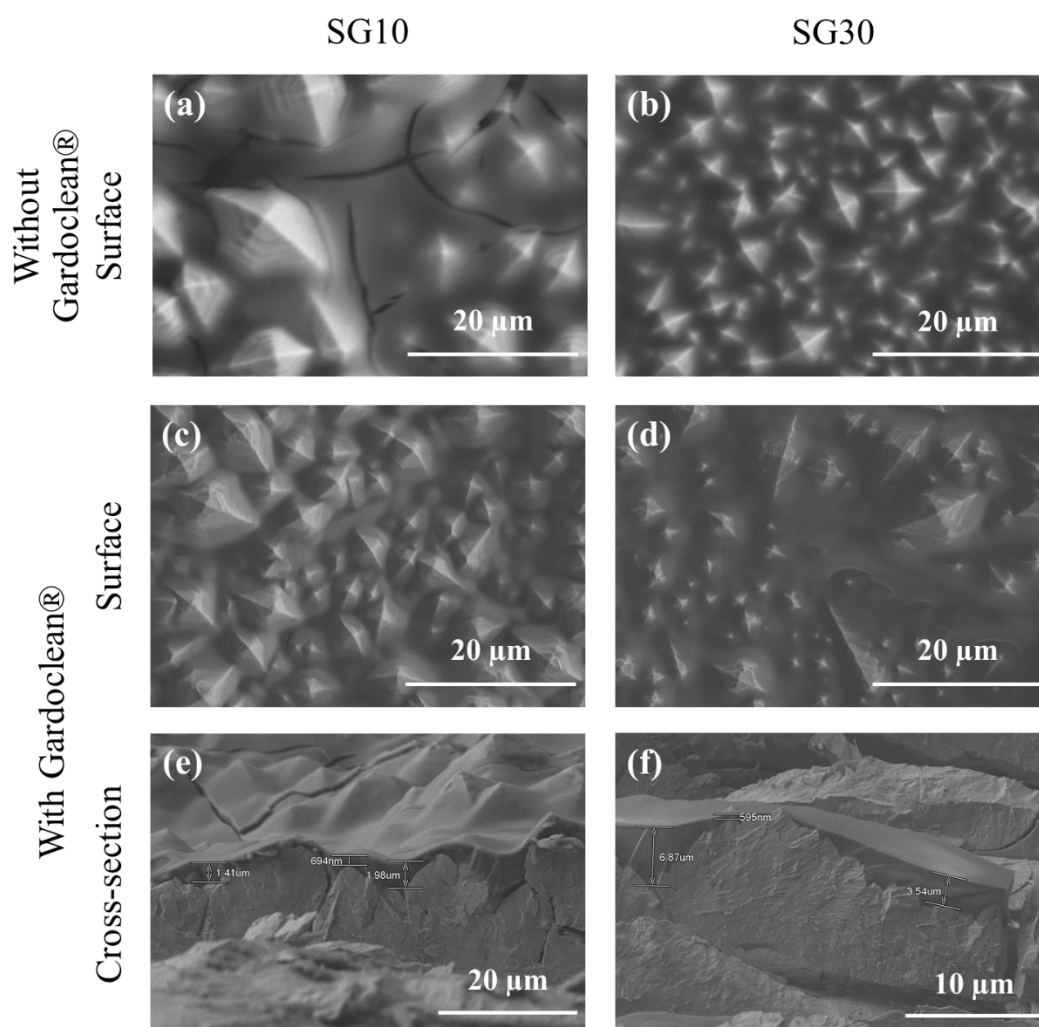

Figure 1. *SEM micrographs of ZnFe deposits with SG10 (without (a) and with Gardoclean® (c and e)) and SG30 (without (b) and with Gardoclean® (d and f)) films. Surface (a, b, c and d) and cross-section (e and f) observations*

$$h = 0.94 \frac{(\eta v_0)^{2/3}}{\gamma_{lv}^{1/6} (\rho g)^{1/2}} \tag{1}$$

where h is the thickness of the film, η is the solution viscosity, v_0 is the withdrawal rate, γ_{lv} is the surface tension and ρg is the gravity parameter. This relation indicates that for the same withdrawal rate, the higher the sol viscosity, the higher the film thickness. This was confirmed by the observation of the cross-section of the samples (Figures 1(e) and (f)). Thickness heterogeneities are observed, particularly between the top (about 1 µm or less) and the bottom of the pyramids (between 2 and 6 µm for SG30). However, the thickness of the film is higher for SG30 (reaching 6 µm).

A decrease in the hydrophily of the ZnFe deposit was observed with the presence of both SG10 and SG30 films. Indeed, the contact angle between the droplet and the ZnFe deposit could not be measured since the droplet immediately spread on the surface of the sample. Thus, the contact angle was assimilated to 0°. However, in the presence of the SG films, this value was superior to 60° depending on the systems, as shown in Table 2. Fedel *et al.* [28] obtained similar values (between 61 and 67°) with an SG film containing 10 % in precursors. Two hypotheses can explain the modification of the hydrophilic behaviour of the systems. First, SG films are composed of GPTMS and MTES. Each of them presents an organic group. Methyl group in MTES could decrease the hydrophilic aspect of the system. Moreover, higher contact angle values were obtained for SG10 films, which could be due to the surface morphology. SEM micrographs (Figure 1) revealed that both SG10 and SG30 films follow the pyramidal shape of the ZnFe deposit. However, fewer pyramid peaks are visible in the case of SG30 film due to the levelling effect of the film. According to the literature, a hydrophobic behaviour can be obtained with a nanostructured morphology [32,33]. Although ZnFe deposits are not nanostructured, the presence of more pyramid peaks for ZnFe + SG10 systems could decrease their hydrophilic behaviour.

Table 2. *Contact angles measured for the different coated systems, with and without Gardoclean®*

	Contact angle, °	
	Without Gardoclean®	With Gardoclean®
SG10	72.2 ± 0.1	76.9 ± 0.3
SG30	62.6 ± 0.5	66.2 ± 0.4

Electrochemical characterization

The OCP was measured during the whole electrochemical experiments. After 3 days of immersion, the OCP value of bare ZnFe was about -0.92 V vs. SCE. The OCP value was stable during the first 3 days of immersion for almost all systems. A shift of the OCP value was observed in the presence of SG films: +0.05 V for ZnFe + Gardoclean® + SG10 and +0.13 and +0.09 V for ZnFe + SG30 without and with Gardoclean®, respectively. These shifts indicate a good covering of the SG films. Because of the similarities in behaviour between ZnFe + SG10 with and without Gardoclean®, only ZnFe + Gardoclean® + SG10 will be considered for the rest of the study. Whereas both ZnFe + SG30 and ZnFe + Gardoclean® + SG30 will be considered.

Corrosion resistance of bare ZnFe

The Bode diagrams obtained during EIS measurements of ZnFe in 0.1 M NaCl are presented in Figure 2. An increase of the low-frequency modulus (Figure 2(a)) until 48 h of immersion is observed (from about 1370 Ω cm² after 6 h until about 4370 Ω cm² after 48 h). Then, the low-frequency modulus decreased, reaching about 2700 Ω cm² after 72 h of immersion. These observations, associated with the shift of the time constant towards lower frequencies on the Bode diagram

(Figure 2(b)), would indicate the formation of corrosion products, which was confirmed by the visual observations after the test (Figure 2(c)). Indeed, the surface of the samples is covered with white/bluish products, which could supposedly form a thin oxide layer.
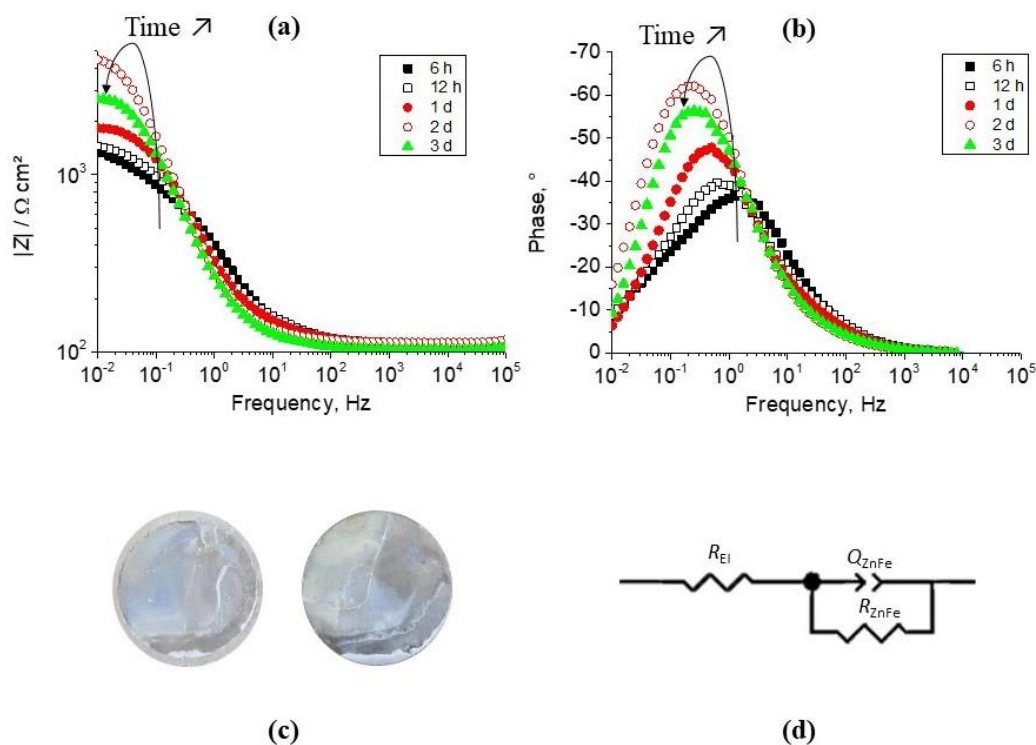

Figure 2. *Evolution of bare ZnFe Bode diagrams in the function of time in 0.1 M NaCl: (a) Modulus diagram and (b) Phase diagram. (c) Visual aspect of the samples after 3 days of immersion in 0.1 M NaCl. The exposed surface is 1 cm². (d) Electrical equivalent circuit used to represent the system*

This electrochemical behaviour can be represented by an electrical equivalent circuit (EEC) (Figure 2(d)) where R_{El} is the electrolyte resistance and Q_{ZnFe} and R_{ZnFe} are associated with the charge transfer at the interface with ZnFe deposit. Data obtained from the EEC (R_{El}, R_{ZnFe}, Q_{ZnFe}, n, which is the CPE parameter and χ^2) are gathered in Table 3. The use of a CPE [34–36] instead of a capacitance describes a non-ideal capacitive behaviour, considering the irregularities of the system (roughness, porosity, adsorption, *etc.*). The impedance of a CPE Z_{CPE} is given by relation (2):

$$Z_{CPE}(\omega) = \frac{1}{Q(j\omega)^n} \tag{2}$$

where Q and n are the CPE parameters. It is possible to calculate the capacitance of a film or a charge transfer with Brug's relation (3) [36].

$$C_{eff} = Q^{1/n}\left(R_e^{-1} + R_t^{-1}\right)^{\frac{-(1-n)}{n}} \tag{3}$$

where C_{eff} if the effective capacitance, Q is the CPE value, R_e is the electrolyte resistance (called R_{El} in this work), R_t is the global resistance and n is the CPE exponent. In our case, $R_t \gg R_e$, consequently, the following relation can be used (4).

$$C_{eff} = Q^{1/n} R_e^{\frac{-(1-n)}{n}} \tag{4}$$

For bare ZnFe, the charge transfer resistance R_t corresponds to R_{ZnFe} (Table 3). This value increases until 2 days of immersion (from 1 kΩ cm² to about 6 kΩ cm²), associated with an increase

in the capacitive aspect of the system (an increase of *n*). Corrosion products could have a barrier effect, thus limiting dissolved oxygen from reaching the surface. After 3 days of immersion, a decrease of R_{ZnFe} is observed until 3 kΩ cm², indicating a rupture of the protecting effect. This could be due to the formation of pulverulent products leading to a loss of adhesion. Moreover, localized corrosion could take place in "less protected" areas. Finally, chloride ions could contribute to the degradation of the protective film formed on ZnFe coating, although they are needed to form some corrosion products (particularly simonkolleite).

Table 3. *Data obtained from the EEC model for the immersion of bare ZnFe in 0.1 M NaCl*

	R_{El} / Ω cm²	R_{ZnFe} / kΩ cm²	Q_{ZnFe} / μF cm⁻² sⁿ⁻¹	n	χ^2 10³
6 h	108	1.22	809	0.68	2.83
12 h	113	1.53	908	0.68	2.11
1 d	117	2.04	862	0.76	4.54
2 d	121	5.96	838	0.85	3.60
3 d	109	3.26	928	0.82	3.77

Influence of the presence of an SG film

Three different systems were investigated: ZnFe + Gardoclean® + SG10 and ZnFe (+ Gardoclean®) + SG30. The Bode diagrams obtained during EIS measurements of the systems in 0.1 M NaCl, the visual aspects of the samples after the tests and the EEC used to represent the systems are presented in Figure 3.

Corrosion resistance of ZnFe + Gardoclean® + SG10

The Bode diagrams obtained during EIS measurements of ZnFe + Gardoclean® + SG10 in 0.1 M NaCl are presented in Figures 3(a) and (b). There is a decrease of the low-frequency modulus after 12 hours of immersion, indicating a loss of barrier properties. On the phase diagram (Figure 3(b)), two time constants were observed until 12 hours of immersion: the high-frequency range associated with the SG film time constant and the middle frequency range associated with the SG/ZnFe interface. After one day of immersion, only one time constant is visible, which is larger than previously and probably corresponds to the gathering of the two time constants. After 2 days of immersion, this time constant is finer and is shifted towards lower frequencies, in the same range as the time constant observed for bare ZnFe after 6 hours of immersion (Figure 2(b)). This shift was also observed for bare ZnFe and was attributed to the formation of corrosion products/oxide layer. At the end of the experiment, the presence of the time constant associated with the SG film can only be supposed.

An EEC with two CPE (Figure 3(h)) was used to represent this system and values are gathered in Table 4. This EEC consists of the electrolyte resistance R_{El}, the SG film characterized by R_{SG} and Q_{SG}. R_2 and Q_2 are associated with the oxide layer formed at the interface between the ZnFe deposit and the SG coating in certain circumstances. In this configuration, the charge transfer resistance R_t would be characterized by R_2. C_{SG} and C_2 (Tables 4, 5 and 6) correspond to the values obtained from Eq. 4 and are effective capacitances. The different resistances R_{El}, R_{SG} and R_2, the effective capacitances C_{SG} and C_2, the CPE parameters n and χ^2 are gathered in Tables 4, 5 and 6 depending on the system. The contribution of the SG film (about 2 kΩ cm² after 6 hours of immersion) is largely inferior to the one of the interfacial oxide layer (about 30 kΩ cm² after 6 h of immersion). These values are consistent with the literature [16,17].

R_{SG} strongly decreases during the first hours of immersion, which is commonly observed in the literature [16,17,19,37,38]. Moreover, the capacitance of this film increases with the immersion time, which could be explained by a water uptake or the break of Si-O-Si bindings.
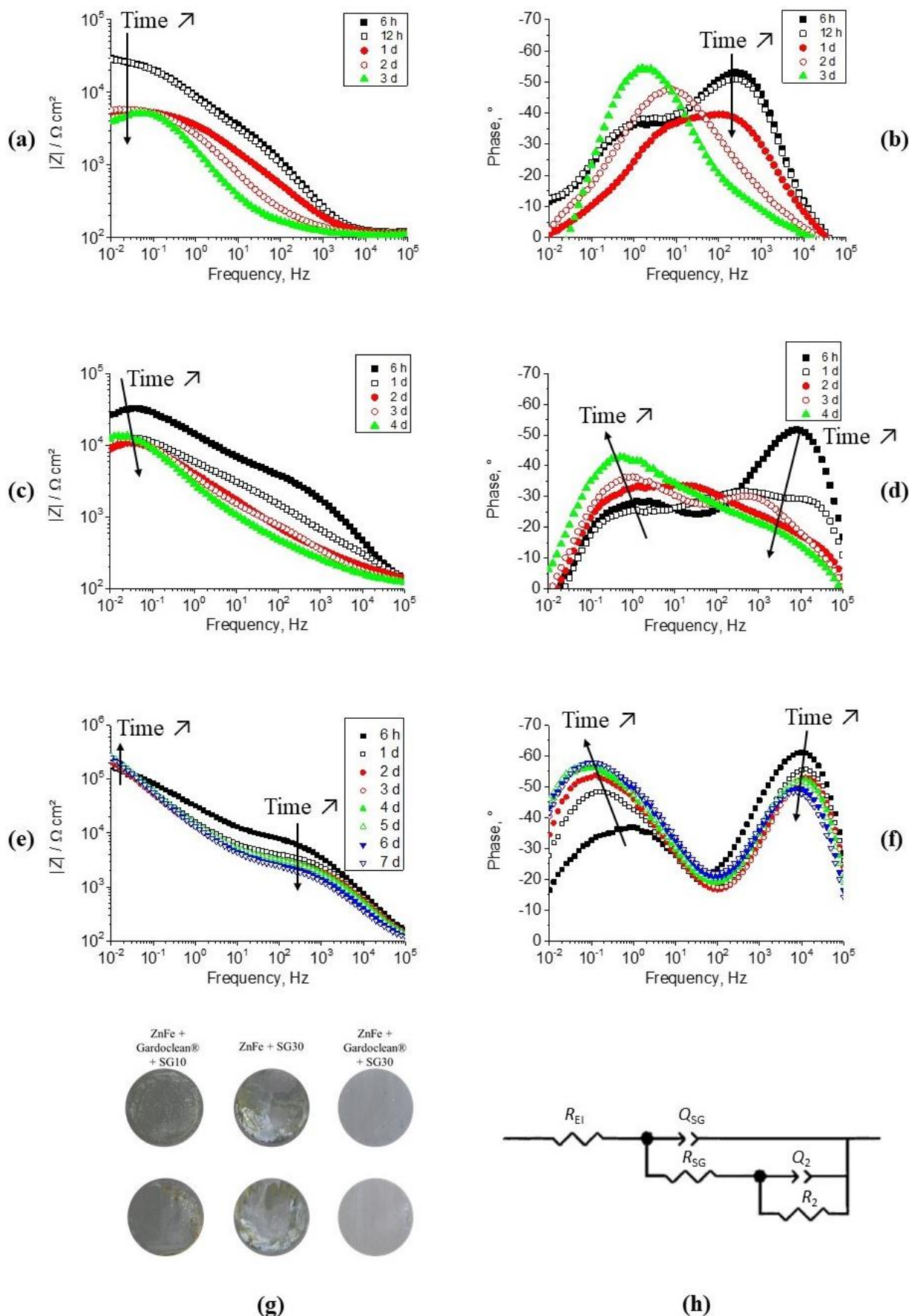
Figure 3. *Evolution of different systems Bode diagrams in function of time in 0.1 M NaCl: (a and b) ZnFe + Gardoclean® + SG10; (c and d) ZnFe + SG30 and (e and f) ZnFe + Gardoclean® + SG30. (g) Visual aspect of the different systems after 3 days (ZnFe + Gardoclean® + SG10) or 7 days (ZnFe (+ Gardoclean®) + SG30) of immersion in 0.1 M NaCl. The exposed surface is 1 cm². (h) EEC used to represent these systems*

A decrease in the oxide layer resistance is also observed and could be attributed to an increase in the exposed surface due to the degradation of the SG film. After 2 days of immersion, C_{SG} and C_2 capacitances are quite high and reach 100 and 25 µF cm⁻². Consequently, a charge transfer phenomenon can be supposed leading to the formation of corrosion products. This hypothesis can be confirmed by the presence of corrosion products on the surface of the sample after 3 days of immersion (Figure 3(g)). These images confirm the improvement in terms of corrosion resistance thanks to the SG film with the presence of intact areas. Corrosion products do not form a homogeneous layer. Indeed, some white/orange points are visible on the surface. The formation of these corrosion products could be explained by the micro-cracks observed in Figure 1(a), allowing the electrolyte to reach the ZnFe deposit.

Table 4. *Data obtained from the EEC model for the immersion of ZnFe + Gardoclean® + SG10 in 0.1 M NaCl*

	R_{El} / Ω cm²	R_{SG} / kΩ cm²	C_{SG} / µF cm⁻²	n	R_2 / kΩ cm²	C_2 / µF cm⁻²	n	$\chi^2\,10^3$
6 h	115	2.54	0.66	0.82	31.81	/	0.56	1.26
12 h	116	2.20	0.72	0.81	32.03	/	0.56	0.63
1 d	113	0.75	1.28	0.75	5.07	/	0.58	0.57
2 d	114	0.09	2.85	0.87	6.19	6.3	0.65	0.89
3 d	110	0.12	108	0.8	5.76	28.8	0.8	2.98

Corrosion resistance of ZnFe + SG30

The Bode diagrams obtained during EIS measurements of ZnFe + SG30 in 0.1 M NaCl until 4 days of immersion are presented in Figures 3(c) and (d). Without Gardoclean® surface preparation, the time constant associated with the SG film strongly decreases during the first hours of immersion, which is consistent with the decrease of the low-frequency modulus. The time constant associated with the ZnFe/SG film interface becomes more intense and is shifted towards lower frequencies. These observations are consistent with the ones obtained for bare ZnFe and ZnFe + Gardoclean® + SG10 and probably indicate the degradation of the SG film and the formation of corrosion products.

This system can be represented by the same EEC as the one used for the system ZnFe + Gardoclean® + SG10. Data obtained from the EEC modelling are gathered in Table 5.

Table 5. *Data obtained from the EEC model for the immersion of ZnFe + SG30 in 0.1 M NaCl*

	R_{El} / Ω cm²	R_{SG} / kΩ cm²	C_{SG} / µF cm⁻²	n	R_2 / kΩ cm²	C_2 / µF cm⁻²	n	$\chi^2\,10^3$
6 h	104	2.08	$5.49.10^{-2}$	0.75	55.57	-	0.53	0.42
12 h	101	2.00	$5.17.10^{-2}$	0.74	55.63	-	0.55	0.73
1 d	105	5.25	-	0.52	17.72	3.77	0.73	0.66
2 d	125	0.51	$8.45.10^{-1}$	0.62	13.92	-	0.59	0.1
3 d	113	0.21	-	0.59	11.12	11.1	0.81	0.21
4 d	109	0.28	1.67	0.60	8.92	6.59	0.66	0.16
5 d	110	0.18	2.33	0.65	12.01	10.4	0.67	0.19
6 d	107	0.12	4.02	0.69	9.75	29.8	0.74	0.69
7 d	103	0.13	2.62	0.67	10.17	25.6	0.72	0.69

R_{SG} values obtained after 6 h of immersion are in the same range as the one obtained previously for ZnFe + Gardoclean® + SG10 (about 2 kΩ cm²). A sharp decrease in this value is observed until 2 days of immersion when it becomes inferior to 1 kΩ cm². The medium/low-frequency time constant was first associated with the interfacial oxide layer (with resistance like the one obtained for ZnFe + Gardoclean® + SG10) and a few µF cm⁻² capacitances. However, the effective capacitance C_2 increases from 3 days of immersion, reaching values superior to 10 µF cm⁻². Consequently, this time constant

was attributed to a charge transfer phenomenon, which could be confirmed by the presence of corrosion products on the surface of the samples (Figure 3(g)). These white/orange corrosion products are spread on most of the surface. Areas with bluish products are also observed and are quite similar to bare ZnFe samples after 3 days of immersion. Finally, areas without corrosion products are detected. SEM observations (Figure 1(b)) highlighted the presence of cracks in the SG films. These cracks could allow the electrolyte to reach the ZnFe deposit, leading to the formation of corrosion products.

Corrosion resistance of ZnFe + Gardoclean® + SG30

The Bode diagrams of ZnFe + Gardoclean® + SG30 are presented in Figures 3(e) and (f). When a Gardoclean® surface preparation is used before the application of the SG film, the time constant associated with the SG film varies essentially during the first day of immersion. This constant slightly decreases while the one associated with the ZnFe/SG film interface increases and is shifted towards lower frequencies. For the first time, the SG film time constant is still observed after 7 days of immersion, indicating the better performance of this system. Finally, the low-frequency modulus is higher than the one obtained for the same system without Gardoclean® and it remains stable during the whole test, indicating the better stability of this system.

The EEC (Figure 3(h)) was used to represent the ZnFe + Gardoclean® + SG30 during the 7 days of immersion and data obtained from the modelling are gathered in Table 6. There is a decrease in R_{SG} during the first days of immersion (from about 7 kΩ cm² after 6 h to about 3 kΩ cm² after 3 days). After 3 days of immersion, this value remains stable. The value obtained after 6 h of immersion is quite higher than the ones obtained for other systems, indicating a great improvement. The effecttive capacitance C_{SG} values are lower than the ones obtained for ZnFe + SG30 (Table 5), indicating two things. First, the corrosion protection provided by this system is better than ZnFe + SG30. Then, the SG film is thicker thanks to the Gardoclean® treatment. Indeed, the capacitance value is inversely proportional to the thickness of the film. The surface preparation could favour the formation of hydroxyl groups on the surface of the ZnFe coating, thus improving the adhesion of the SG film. Moreover, an increase in the C_{SG} values is observed with the immersion time, which is consistent with results obtained for other systems.

Table 6. *Data obtained from the EEC model for the immersion of ZnFe + Gardoclean® + SG30 in 0.1 M NaCl*

	R_{El} / Ω cm²	R_{SG} / kΩ cm²	C_{SG} / nF cm⁻²	n	R_2 / kΩ cm²	C_2 / μF cm⁻²	n	χ^2 10³
6 h	111	6.92	15.3	0.83	241.12	/	0.55	1.25
12 h	112	6.11	1..8	0.82	323.69	/	0.58	1.27
1 d	104	3.74	17.9	0.81	365.55	0.61	0.63	1.6
2 d	100	2.99	18.7	0.79	538.64	1.11	0.66	2.69
3 d	98	2.68	20.6	0.79	946.97	1.11	0.66	2.76
4 d	100	3.10	21.8	0.78	1142.30	0.97	0.66	2.56
5 d	100	3.15	24.0	0.77	1486.60	0.91	0.66	2.41
6 d	96	2.49	28.7	0.76	976.87	1.13	0.67	2.19
7 d	95	2.40	33.5	0.75	832.02	1.25	0.68	2.25

Regarding corrosion resistance, the contribution of the SG film is largely inferior to the one of the interfacial oxide layer. Indeed, its resistance is superior to 240 kΩ cm² compared to about 7 kΩ cm² for the SG film. The effective capacitance C_2 of this layer is about 1 μF cm⁻² during the whole test, indicating the absence of charge transfer. In this case, the oxide layer resistance R_2 increases during the first days of immersion. This could be explained by an electrolyte infiltration reaching the oxide

layer and/or ZnFe deposit. The formation of oxides could reinforce the existing oxide layer and seal micro-defects in the SG film. This hypothesis could illustrate, on the one hand, the increase of the oxide layer resistance and, on the other hand, the stabilization of the SG film resistance.

After 7 days of immersion, the surface of the samples is quite intact, showing that the combination of Gardoclean® treatment and SG30 film considerably limits the degradation of ZnFe electrodeposit.

SEM observations after 7 days of immersion are presented in Figure 4 for the ZnFe + Gardoclean® + SG30 configuration. The SG film is observed on the whole exposed area. Moreover, ZnFe pyramids (red circles in Figure 4) are still visible under the SG film. A micro-crack (orange rectangle) is detected and could permit the infiltration of electrolytes and the formation of corrosion products. Indeed, some corrosion products are present on the SEM micrograph. However, they were not distinguished by the naked eye.
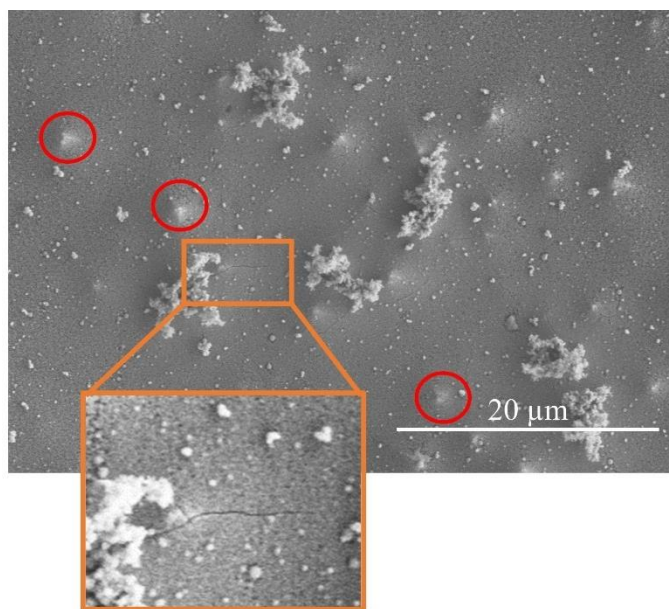
Figure 4. *SEM micrograph of a ZnFe + Gardoclean® + SG30 after 7 days of immersion in 0.1 M NaCl. The red circles indicate the presence of ZnFe pyramids. The orange rectangle highlights the presence of cracks in the SG film*

Comparison of the different systems

The evolution of the low-frequency modulus of bare ZnFe, ZnFe + Gardoclean® + SG10 and ZnFe + SG30 (with and without Gardoclean® surface preparation) is presented in Figure 5. Several areas were drawn, corresponding to different behaviours.

The area I is associated with bare ZnFe. The low-frequency modulus increases until 2 days of immersion and then decreases until 3 days. The increase of the low-frequency modulus was attributed to the formation of corrosion products, while the decrease was explained by a loss of the protective aspect provided by these corrosion products.

Area II corresponds to the systems ZnFe + Gardoclean® + SG10 and ZnFe + SG30. During the first 12 hours of immersion, a great increase of the low-frequency modulus is observed, in comparison with bare ZnFe, indicating the barrier properties of the SG films. In this area, the low-frequency modulus rapidly decreases during the first 24 hours of immersion and then remains stable until 3 days of immersion. This evolution shows a loss of barrier properties associated with the SG film. Although the low-frequency modulus is superior to the one of bare ZnFe, the presence of corrosion products on the surface of the samples highlights the lack of corrosion resistance.
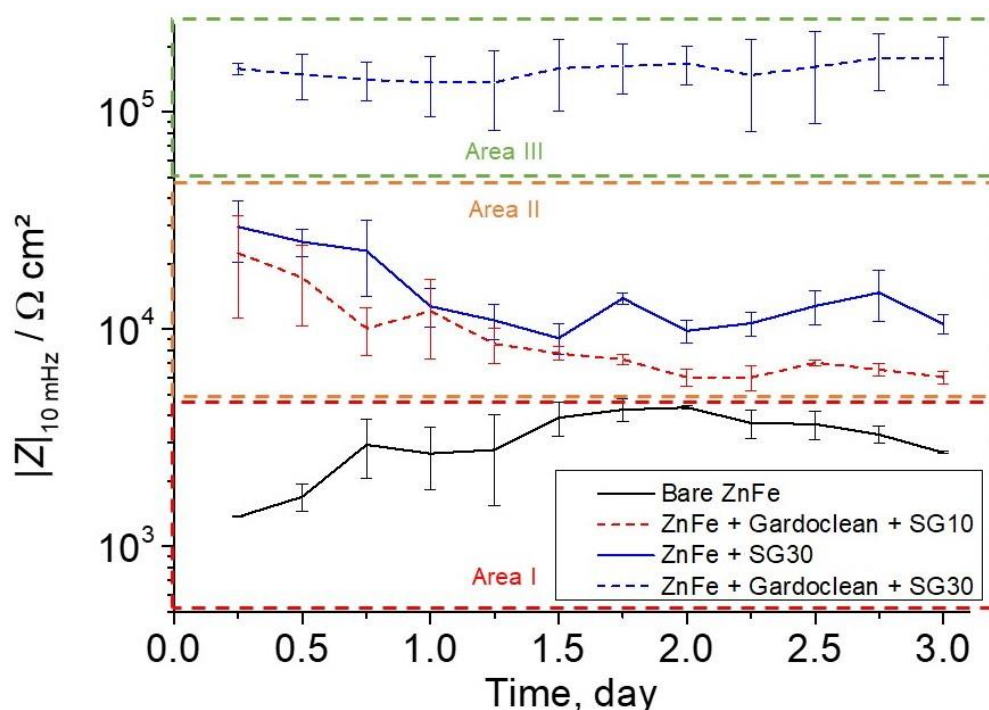
Figure 5. *Evolution of the low-frequency modulus in the function of the immersion time in 0.1 M NaCl for bare ZnFe, ZnFe + Gardoclean® + SG10 and ZnFe + SG30 with and without Gardoclean®*

Finally, the evolution of ZnFe + Gardoclean® + SG30 is shown in area III. An increase of two decades in terms of low-frequency modulus is noted after 6 hours of immersion, in comparison with bare ZnFe. Moreover, this value remains quite constant until 3 days of immersion, indicating the good corrosion protection provided by this system.

Salt spray test

The evolution of bare ZnFe, ZnFe + Gardoclean® + SG10 and ZnFe + SG30 with and without Gardoclean® surface preparation after several days of neutral salt spray test is presented in Figure 6. Usually, two times are determined during Zn coated steel exposed to salt spray test: the time before white rust appearance, the time before red rust appearance. However, in the case of ZnFe coatings, the appearance of red rust is not associated with the corrosion of the steel substrate. Indeed, the degradation of the ZnFe deposit leads to the formation of iron and/or zinc products which are respectively red and white. Visually, it is impossible to distinguish red corrosion products obtained from the corrosion of the ZnFe deposit from those obtained from the corrosion of the steel substrate.

Behaviour of bare ZnFe exposed to NSS

Figure 6 shows that corrosion products, mostly white, are formed from the first day of exposure. These products are supposedly formed due to the dissolution of zinc from the ZnFe deposit. Few orange areas are visible, but they become more intense after several days of exposure. After 7 days, iron corrosion products are majoritarian and form a voluminous layer. Some of the corrosion products fell when samples were dried, indicating their lack of adhesion. SEM observation of samples after different times of exposure permitted to identify corrosion products. Figure 7 represents SEM micrographs obtained for the different systems after different times of exposure. For bare ZnFe, after 3 and 7 days of exposure (Figure 7(a) and (b) respectively), corrosion products with different morphologies were observed. Hexagonal crystals could be associated with zinc corrosion products. Among them, simonkolleite ($Zn_5(OH)_8Cl_2.H_2O$) presents hexagonal crystals [39,40].
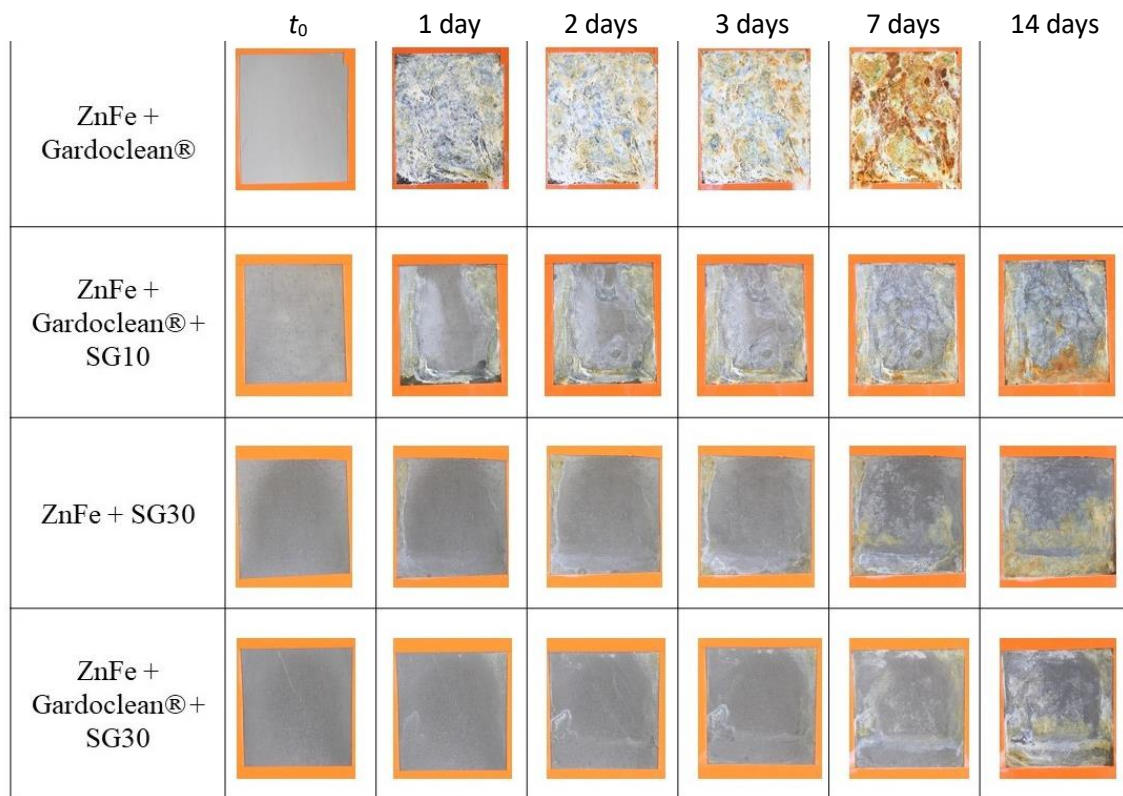
Figure 6. *Evolution of the visual aspect of bare ZnFe, ZnFe + Gardoclean® + SG10 and ZnFe + SG30 with and without Gardoclean®, after different days of exposure in the NSS test*
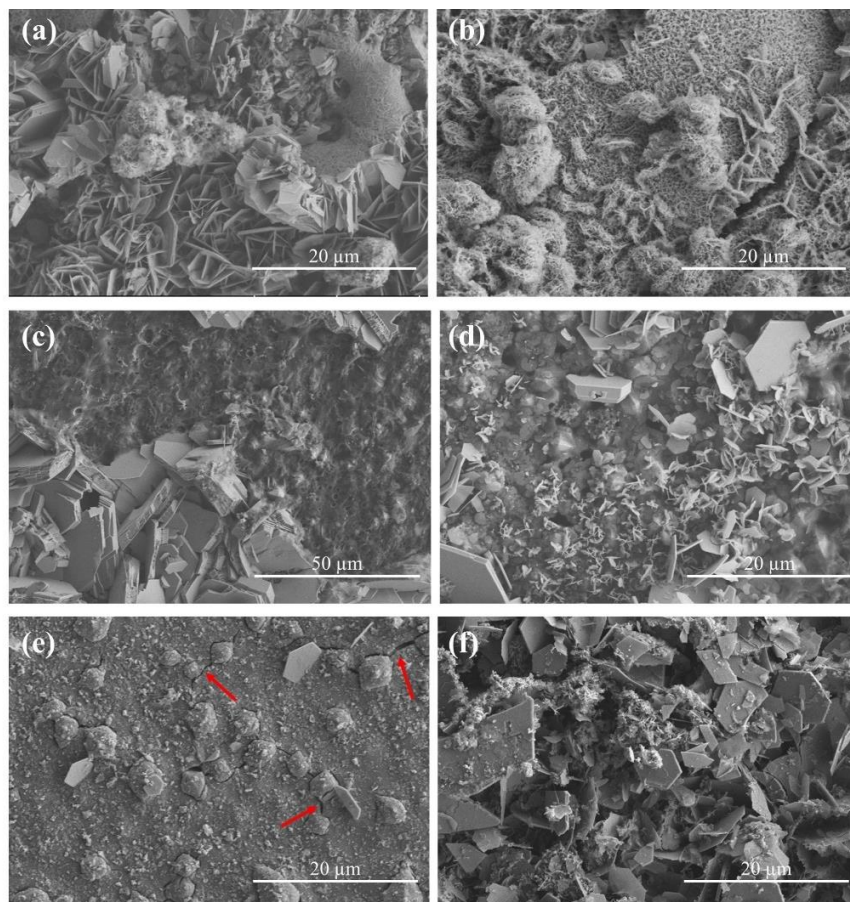

Figure 7. *SEM micrographs of the different systems after exposure to NSS test: (a and b) Bare ZnFe after 3 and 7 days of exposure, respectively; (c and d) ZnFe + Gardoclean® + SG10 after 14 days of exposure and (e and f) ZnFe + Gardoclean® + SG30 after 7 days of exposure*

Behaviour of ZnFe + Gardoclean® + SG10 exposed to NSS

The surface of ZnFe + Gardoclean® + SG10 is covered in corrosion products after only 1 day of exposure (Figure 6). Corrosion products are mostly white, but some orange areas are observed and become more present when exposure time increases. This result is consistent with the Bode diagram evolution (Figures 3(a) and (b)). Indeed, it showed a large decrease in the SG film resistance (R_{SG}) during the first 12 hours of immersion in 0.1 M NaCl. Moreover, SEM micrographs (Figure 1) revealed the presence of cracks in the SG deposit associated with small thicknesses (<1 µm) locally. However, the corrosion products layer seems less thick than on bare ZnFe. Moreover, the system seemed quite stable until 3 days of exposure with few evolutions from day 1 to day 3, indicating that the SG film slows down the formation of corrosion products. After 7 days of exposure, the benefits of the SG films are perfectly visible since the corrosion products layer is far more important on bare ZnFe. Figures 7(c) and (d) show the surface of the ZnFe + Gardoclean® + SG10 system after 14 days of exposure, observed by SEM. Hexagonal crystals are observed with different thicknesses. Figure 7(c) highlights the presence of pyramidal grains associated with the ZnFe coating. An EDX mapping of this Figure 7(c) is presented in Figure 8, where area 1 corresponds to hexagonal crystals while area 2 is associated with pyramidal grains. The EDX mapping confirmed that area 2 was still protected with the presence of Si and the detection of Fe. However, area 1 is rich in O and Cl and Fe and Si are almost not detected. These results could indicate a degradation of the SG film and thus the corrosion of the ZnFe deposit, leading to the formation of corrosion products. Finally, the formation of simonkolleite could be supposed due to the hexagonal shape of the crystals and the presence of Cl.
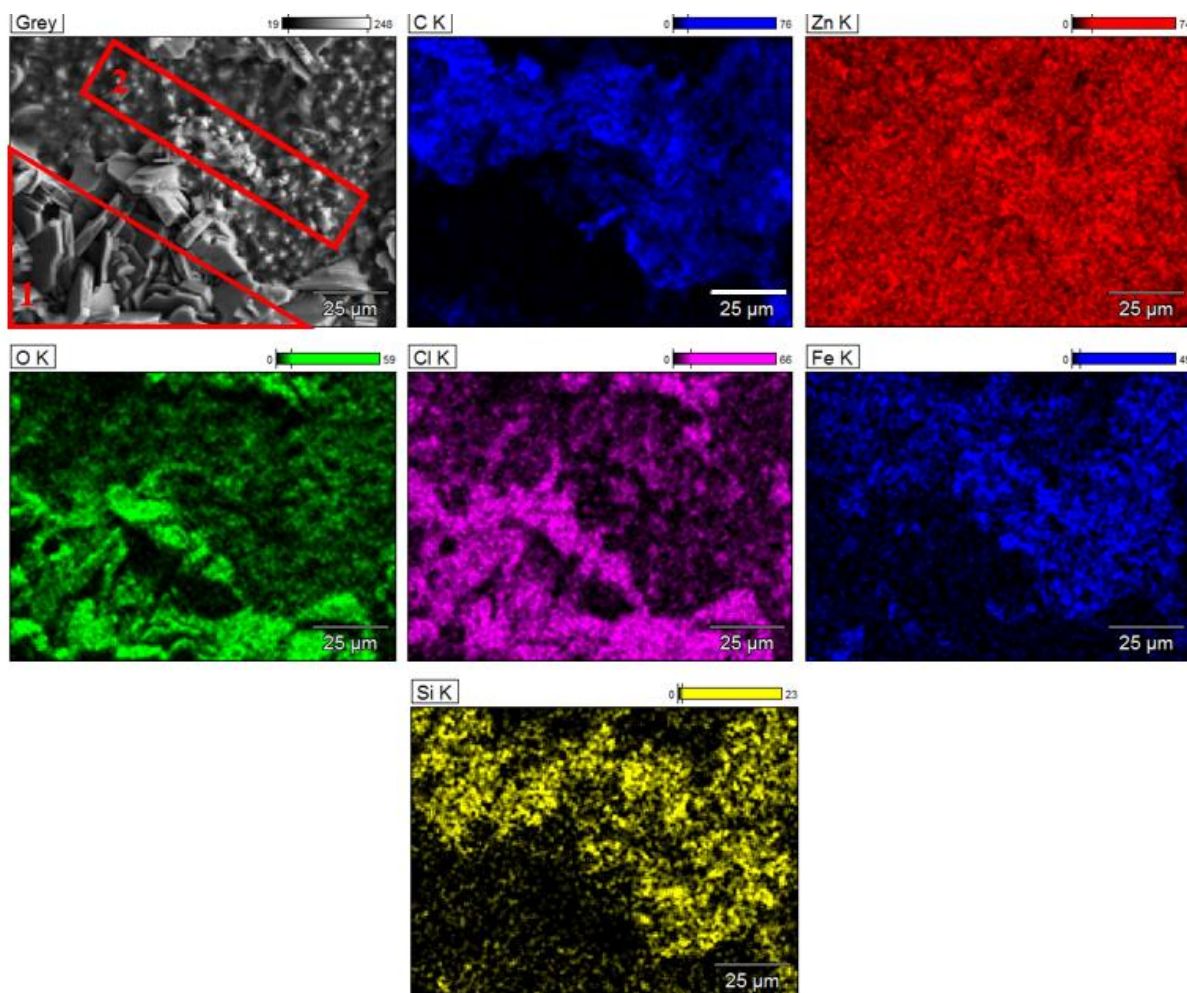

Figure 8. *EDX mapping ZnFe + Gardoclean® + SG10 after 14 days of exposure (Figure 7 (c))*

Behaviour of ZnFe + SG30 with and without Gardoclean®

Figure 6 reveals an improvement in the corrosion resistance with the ZnFe + SG30 systems. Indeed, few corrosion products are observed on the surface of the samples until 3 days of exposure. After 14 days of exposure, most of the surface is covered by orange corrosion products. However, the SG film considerably limits the formation of corrosion products since samples are less corroded after 14 days of exposure than bare ZnFe after 1 day of exposure. Contrary to EIS results, no improvement due to Gardoclean® treatment was observed, which could be explained by the aggressiveness of the test. The SEM observations of the surface of ZnFe + Gardoclean® + SG30 after 7 days of immersion are presented in Figures 7(e) and (f). Figure 7(e) reveals the presence of hexagonal crystals that go through the SG film, which presents some cracks (indicated by red arrows). Figure 7(f) shows an area entirely covered with corrosion products, mainly hexagonal crystals. Similar products were observed for ZnFe + Gardoclean® + SG10.

Conclusions

An aqueous SG film composed of TEOS, MTES and GPTMS was deposited on ZnFe coated steel. Due to the pyramidal shape of the ZnFe electrodeposit, cracks were observed in the SG films. However, the use of an alkaline surface preparation permitted to limit this phenomenon. Thickness heterogeneities were also observed due to this pyramidal shape. Electrochemical tests highlighted an improvement of the corrosion resistance of ZnFe deposit thanks to the SG films, with an increase of the low-frequency modulus. But this effect lasted only for the system ZnFe + Gardoclean® + SG30 showing a higher precursor content, which remained stable during 7 days of immersion in 0.1 M NaCl. The same conclusions were obtained with an NSS test, showing that the systems ZnFe (+ Gardoclean®) + SG30 are the most promising solution, with the absence of corrosion products until 3 days of exposure.

References

[1]   D. Marchandise, J. M. Cuntz, J. Creus, M. Gavrila, C. Rothea, H. Idrissi, J. P. Millet, *Matériaux & Techniques* **85(5-6)** (1997) 33-38. https://doi.org/(10.1051/mattech/199785050033

[2]   M. Gavrila, J. P. Millet, H. Mazille, D. Marchandise, J. M. Cuntz, *Surface and Coatings Technology* **123** (2000) 164-172. https://doi.org/10.1016/S0257-8972(99)00455-7

[3]   European Chemicals Agency. https://echa.europa.eu/documents/10162/3bbe9024-52a6-8e63-5581-e686331eb459 (accessed April 16, 2022).

[4]   C. J. Lan, W. Y. Liu, T. S. Chin, *Journal of The Electrochemical Society* **154** (2007) D30. https://doi.org/10.1149/1.2393011

[5]   C. J. Lan, W. Y. Liu, S. T. Ke, T. S. Chin, *Surface and Coatings Technology* **201** (2006) 3103–3108. https://doi.org/10.1016/j.surfcoat.2006.06.027

[6]   J. B. Bajat, V. B. Mišković-Stanković, M. D. Maksimović, D. M. Dražić, S. Zec, *Journal of the Serbian Chemical Society* **69** (2004) 807-815. https://doi.org/10.2298/JSC0410807B

[7]   K. O. Nayana, T. V. Venkatesha, K. G. Chandrappa, *Surface and Coatings Technology* **235** (2013) 461-468. https://doi.org/10.1016/j.surfcoat.2013.08.003

[8]   R. S. Bhat, A. C. Hegde, *Analytical & Bioanalytical Electrochemistry* **4** (2012) 593-609.

[9]   H. Park, J. A. Szpunar, *Corrosion Science* **40** (1998) 525-545. https://doi.org/10.1016/S0010-938X(97)00148-0

[10]   H. L. Hu, Y .M. Zhu, Z. M. Tu, W. J. Liu, *Advanced Materials Research* **194–196** (2011) 2209-2215. https://doi.org/10.4028/www.scientific.net/AMR.194-196.2209

[11]   H. Y. Su, P. L. Chen, C. S. Lin, *Corrosion Science* **102** (2016) 63-71. https://doi.org/10.1016/j.corsci.2015.09.019

[12]   E. Volentiru, M. Nyári, G. Szabó, Z. Hórvölgyi, L. M. Murşan, *Periodica Polytechnica Chemical Engineering* **58** (2014) 61-66. https://doi.org/10.3311/PPch.7302

[13]   M. Garcia-Heras, A. Jimenez-Morales, B. Casal, J. C. Galvan, S. Radzki, M. A. Villegas, *Journal of Alloys and Compounds* **380** (2004) 219-224. https://doi.org/10.1016/j.jallcom.2004.03.047

[14]   V. Meiffren, K. Dumont, P. Lenormand, F. Ansart, S. Manov, *Progress in Organic Coatings* **71** (2011) 329-335. https://doi.org/10.1016/j.porgcoat.2011.03.025

[15]   M. Mayrand, J. F. Quinson, A. Roche, V. Roisne, H. Guyon, *Journal of Sol-Gel Science and Technology* **12** (1998) 49-57. https://doi.org/10.1023/A:1008605110207

[16]   M. Fedel, E. Callone, S. Diré, F. Deflorian, M. G. Olivier, M. Poelman, *Electrochimica Acta* **124** (2014) 90-99. https://doi.org/10.1016/j.electacta.2013.11.006

[17]   M. Poelman, M. Fedel, C. Motte, D. Lahem, T. Urios, Y. Paint, F. Deflorian, M. G. Olivier, *Surface and Coatings Technology* **274** (2015) 1-8. https://doi.org/10.1016/j.surfcoat.2014.06.021

[18]   M. F. Montemor, R. Pinto, M. G. S. Ferreira, *Electrochimica Acta* **54** (2009) 5179-5189. https://doi.org/10.1016/j.electacta.2009.01.053

[19]   W. Trabelsi, P. Cecilio, M. G. S. Ferreira, M. F. Montemor, *Progress in Organic Coatings* **54** (2005) 276-284. https://doi.org/10.1016/j.porgcoat.2005.07.006

[20]   M. Fedel, M. Poelman, M. Zago, C. Vandermiers, D. Cossement, M. G. Olivier, F. Deflorian, *Surface and Coatings Technology* **274** (2015) 9-17. https://doi.org/10.1016/j.surfcoat.2014.07.020

[21]   S. Bera, T. K. Rout, G. Udayabhanu, R. Narayan, *Progress in Organic Coatings* **101** (2016) 24-44. https://doi.org/10.1016/j.porgcoat.2016.07.010

[22]   R. Z. Zand, K. Verbeken, A. Adriaens, *International Journal of Electrochemical Science* **8** (2013) 548-563.

[23]   G. Kong, J. Lu, H. Wu, *Journal of Rare Earths* **27** (2009) 164-168. https://doi.org/10.1016/S1002-0721(08)60213-6

[24]   A. M. Cabral, W. Trabelsi, R. Serra, M. F. Montemor, M. L. Zheludkevich, M. G. S. Ferreira, *Corrosion Science* **48** (2006) 3740-3758. https://doi.org/10.1016/j.corsci.2006.01.010

[25]   M. G. S. Ferreira, R. G. Duarte, M. F. Montemor, A. M. P. Simões, *Electrochimica Acta* **49** (2004) 2927-2935. https://doi.org/10.1016/j.electacta.2004.01.051

[26]   M. C. G. dos Santos, C. M. A. Freire, *Revista Materia* **18** (2013) 1576-1586. https://doi.org/10.1590/S1517-70762013000400017 (In Portuguese)

[27]   M. Fedel, M. E. Druart, M. Olivier, M. Poelman, F. Deflorian, S. Rossi, *Progress in Organic Coatings* **69** (2010) 118-125. https://doi.org/10.1016/j.porgcoat.2010.04.003

[28]   M. Fedel, M. Olivier, M. Poelman, F. Deflorian, S. Rossi, M. E. Druart, *Progress in Organic Coatings* **66** (2009) 118-128. https://doi.org/10.1016/j.porgcoat.2009.06.011

[29]   C. Motte, Etude de la protection contre la corrosion de l'acier galvanisé en continu par un revêtement sol-gel modifié par des nano-argiles - Thèse de doctorat, Université de Mons, 2012. (in French)

[30]   A. Nicolay, Elaboration et caractérisation de revêtements nanocomposites hybrides nano-particules/sol-gel multifonctionnels - Thèse de doctorat, Université de Mons, 2017. (in French)

[31]   C. Arrighi, C. Savall, S. Cohendoz, J.L. Grosseau-Poussard, L. Baissac, M. G. Olivier, J. Creus, *Materials Chemistry and Physics* **263** (2021) 124366. https://doi.org/10.1016/j.matchemphys.2021.124366

[32]   Y. Qing, C. Yang, Z. Yu, Z. Zhang, Q. Hu, C. Liu, *Journal of The Electrochemical Society* **163** (2016) D385-D391. https://doi.org/10.1149/2.0571608jes

[33]   Y. Qing, C. Hu, C. Yang, K. An, F. Tang, J. Tan, C. Liu, *ACS Applied Materials and Interfaces* **9** (2017) 16571-16580. https://doi.org/10.1021/acsami.6b15745

[34]   B. Hirschorn, M. E. Orazem, B. Tribollet, V. Vivier, I. Frateur, M. Musiani, *Electrochimica Acta* **55** (2010) 6218-6227. https://doi.org/10.1016/j.electacta.2009.10.065

[35]   M. N. Kakaei, J. Neshati, A. R. Rezaierod, *Protection of Metals and Physical Chemistry of Surfaces* **54** (2018) 548-556. https://doi.org/10.1134/S2070205118030280

[36]   G. J. Brug, A. L. G. van den Eeden, M. Sluyters-Rehbach, J. H. Sluyters, *Journal of Electro-analytical Chemistry* **176** (1984) 275-295. https://doi.org/10.1016/S0022-0728(84)80324-1

[37]   M. F. Montemor, M. G. S. Ferreira, *Electrochimica Acta* **52** (2007) 6976-6987. https://doi.org/10.1016/j.electacta.2007.05.022

[38]   C. Agustín-Sáenz, E. Martín-Ugarte, J. B. Jorcin, G. Imbuluzqueta, P. Santa Coloma, U. Izagirre-Etxeberria, *Journal of Sol-Gel Science and Technology* **89** (2019) 264-283. https://doi.org/10.1007/s10971-018-4840-6

[39]   G. Kirov, S. Dencheva, *Comptes Rendus de l'Académie Bulgare Des Sciences* **69(2)** (2016) 169-176.

[40]   S. Cousy, N. Gorodylova, L. Svoboda, J. Zelenka, *Chemical Papers* **71** (2017) 2325-2334. https://doi.org/10.1007/s11696-017-0226-4